DNA tetrahedron-Au NPs-GO for enhanced fluorescence detection of serotonin

Zhang Yun [a,*], Wu Qiong [a], Gao Hui [a], Zhang Hua [a], Miao Xiang-Min [b]

[a] Changzhi Key Laboratory of Drug Molecular Design and Innovative Pharmaceutics, School of Pharmacy, Changzhi Medical College, Changzhi, Shanxi 046000, PR China
[b] School of Life Science, Jiangsu Normal University, Xuzhou 221116, PR China

Abstract

Evidence had accumulated that serotonin (5-HT), a hormone and neurotransmitter, was not only involved in a variety of different physiological and central nervous system functions but also in the development and manifestation of psychiatric diseases. Here, DNA tetrahedron-Au NPs-GO for enhanced fluorescence sensor was designed for detecting serotonin. Au NPs-GO was used as a fluorescence quencher, while fluorophore-labeled DNA tetrahedron was used as a donor, resulting in fluorescence resonance energy transfer (FRET) from the fluorophore to Au NPs-GO (signal off). With the strong binding ability of aptamer to serotonin, S5 was released from Aptamer: S5 duplex, then reacted with the tail of DNA tetrahedron (DTNs), followed by the formation of three double stranded DNA products in the tail of DTNs, bringing in signal readout responses (signal on). Consequently, a reliable, sensitive and selective sensor was obtained for one-step quantificative detection of serotonin from 50 pM to 200 nM with a detection limit of 16.8 pM. Furthermore, satisfactory stability, reproducibility, specificity and good recovery efficiency in human serum samples revealed that the proposed sensor could be served as a prospective tool for serotonin detection.

Keywords: Au NPs-GO, DNA tetrahedron, Fluorescence, One-step, Serotonin

1. Introduction

Serotonin (5-hydroxytryptamine, 5-HT) is a monoamine, an important biomolecule in physiological systems, a neurotransmitter widely dispersed throughout the central nervous system, playing a crucial role in temperature regulation, muscle contraction, liver regeneration, endocrine regulation, mood, sleep, emesis, sexuality, and appetite [1−3]. However, the level of serotonin in the human body has a significant impact on life and health. An excessively high level of serotonin is manifested toxicity, liver regeneration, thermoregulation and irritable bowel syndrome. Meanwhile, a too low level of serotonin can lead to depression, infantile autism, Alzheimer's disease, carcinoid syndrome, migraines, mental retardation, sudden infant death syndrome, sleep disorders, sexual dysfunction, and Parkinson's disease [4,5]. Thus, it is necessary to find an easy, sensitive and selective method to detect serotonin in diagnosing some diseases, and aid in understanding the role of serotonin in some neurological disorders.

Effective monitoring of serotonin is highly dependent on reliable analytical methods. At present, detection of serotonin can be performed using a variety of techniques such as electrochemistry [6,7], electrochemiluminescence [8,9], colorimetry [10], and surface enhanced Raman scattering [11], fluorescence [12,13]. Among which, fluorescence-based detection system has been extensively employed in bioanalysis, due to their advantages of high sensitivity, selectivity, fast analysis, cost-effectiveness, and ease of operation [14,15].

As a class of novel fluorescence quenching nanomaterial, graphene oxide (GO) nanomaterials

Received 8 August 2025; accepted 29 October 2025.
Available online 15 December 2025

* Corresponding author.
E-mail address: zhangyun0320@126.com (Z. Yun).

https://doi.org/10.38212/2224-6614.3572

have attracted tremendous attentions in recent years owing to its high surface area and ability to hold conductive nanoparticles [16,17]. It is commonly applied in biosensing [18], antimicrobial [19] and bioimaging [20] fields. Moreover, GO functionalized by nanoparticle possesses unique physical and chemical properties, such as hypersensitivity and excellent catalytic performance, and it can increase the available surface area for the combination of analytes. Such characteristics make GO-nanoparticles composites have potential application value in the preparation of optical biosensors [21]. Therefore, GO modified by Au nanoparticles through electrostatic interaction between the negative charge on the surface of GO and the positive charge of Au ions (Au NPs-GO) can greatly enhance the surface area for more DNA probe's immobilization. In addition, fluorophore labeled single-stranded DNA (ssDNA) probes could adsorb onto the surface of GO, accompanied with the quenching of fluorescence signals.

DNA tetrahedron (DTNs) is a typical and simple three-dimensional DNA nanostructure, because it has incomparable advantages compared with other DNA structures like simple preparation, good stability, unique cavity structure, and strong anti-degradation performance [22–24]. Meanwhile, functional groups can be systematically arranged on the DTNs, thereby enhancing their functional properties. Now, it is widely used in biosensing, cargo loading in biomedicine, and bioimaging with these excellent properties [25–28].

In view of the above points, an ultrasensitive and switch-on sensor was developed for serotonin detection by using Au NPs-GO as a novel fluorescence quenching platform. As outlined in Scheme 1, the fluorescence of 6-carboxyfluorescein (FAM) modified S2, S3 and S4 of DTNs were both quenched by Au NPs-GO because of FRET effect from fluorescence molecules (donor) to Au NPs-GO (quencher), inducing fluorescence signal off. When target serotonin presented, the aptamer specifically recognized with serotonin and S5 was released (Scheme 1A). Subsequently, S5 was hybridized with S2, S3 and S4 of DTNs, leading to the formation of double stranded DNA product (Scheme 1B). Consequently, the robustness of double stranded DNA eliminated the adsorption effect of Au NPs-GO, and the fluorescence response of FAM at 521 nm was obtained.

2. Materials and methods

2.1. Materials

Chloroauric acid ($HAuCl_4$), Sodium borohydride ($NaBH_4$), and CTAB were purchased from Aladdin Biotech CO. Ltd. (Beijing, China). Graphene oxide was purchased from Nanjing XFNano Mstar Technology. Ltd. (Nanjing, China). All other reagents

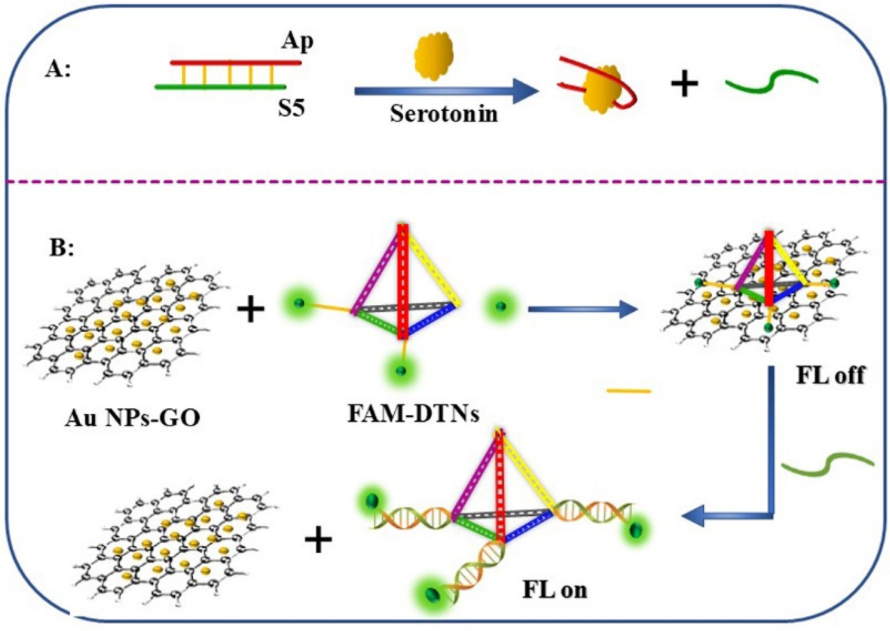

Scheme 1. DNA tetrahedron-based fluorescence sensor for serotonin detection.

used in this work were of analytical grade. The ultrapure water used in the experiments was prepared using a Milli-Q system (Merck Millipore, USA). DNA oligonucleotides with different sequences were synthesized by Sangon Biological Engineering Technology & Services Co. Ltd. (Shanghai, China) and the corresponding DNA sequences were shown in Table 1.

2.2. Apparatus

F-4600 spectrophotometer (HITACHI, Japan) was employed to characterize the fluorescence response of the sensor. The morphology of GO and Au NPs-GO was characterized using scanning electron microscopy (SEM, JSM-6330F microanalyzer, JEOL, Japan) and using the transmission electron micrograph (TEM, JEM-2100F microscope). The chemical composition and valence states of Au NPs-GO were determined by X-ray photoelectron spectroscopy (XPS) on an ESCALAB 250XI instrument (Thermo Fisher Scientific Inc., Pittsburgh, PA, USA). UV-vis absorption spectrum of GO and Au NPs-GO was recorded using a UV spectrophotometer (Shimadzu Co. Kyoto, Japan).

2.3. Synthesis of AuNPs

AuNPs were synthesized according to the literature method [29]. Firstly, 15 mL of $HAuCl_4$ (1.0 mM) and 2 mL of CTAB (10 nM) were mixed, and followed by adding 2 mL of $NaBH_4$ (100 mM) and stirred continuously until the color of the solution changed to orange red. Then, the prepared Au NPs were stored at 4 °C before using.

2.4. Preparation of Au NPs-GO

Au NPs-GO were prepared according to the literature method [30]. Typically, 25 mL of Au NPs (0.48 mM) was mixed with 1.25 mL of GO solution (1 mg/mL). After that, the mixture was stirred for 30 min with bath heating at 80 °C. After incubating for 60 min, the mixture was centrifuged at 5000 rpm for 15 min, and the resultant composite was washed with distilled water to remove the free gold nanoparticles (Au NPs). Meanwhile, the concentration of Au NPs that modified onto GO surface was evaluated according to the literature method [31], with a concentration of 1.8 nM. The prepared Au NPs-GO were stored in 4 °C before using.

2.5. Synthesis of DTNs

S1 and the other three DNA strands modified by FAM (S2, S3 and S4) were all dissolved in 20 mM PBS buffer (pH 8.0, containing 5.0 mM Mg^{2+}) with a final concentration of 2 μM. The resulting mixture was heated at 95 °C for 5 min and then cooled to room temperature. The formed DTNs was stored in 4 °C before using.

2.6. Gel analysis of DTNs

Agarose gel electrophoresis was carried out to confirm the happen of DTNs. Firstly, 1.5 wt% agarose gel was prepared and 4.0 μL of different DNA samples (1.0 μM) were loaded into the lanes. After that, the gel electrophoresis was performed by using 1.0 × TAE as running buffer at a constant potential of 84 V for 55 min. After Stains-All staining by EB solution for 15 min, the gels were photographed by using the gel image system.

2.7. Fluorescent detection procedure of serotonin

To realize the quantitative detection of serotonin, 0.5 μM aptamer and 0.5 μM S5 were firstly hybridized to the double-stranded strands. Then, varying concentrations of serotonin were added and happened a competitive response with aptamer. After that, above reaction products were added 200 μL of Au NPs-GO solution (0.15 mg/mL) and incubated for 50 min at 37 °C, the fluorescence

Table 1. Sequences of DNA employed in this work.

Name	Sequences (5′–3′)
S1	ACATTCCTCAGTCTGCTGTCCAGCAGAGCGTTATGACAGCTTGCTACACGCCCTATTAGCGATTG AAGAGCCGTAGCGAGTATACGTTACTTAG
S2	TATCAGCAGGCAGTTGACGCGACAGTCGCGTTTCGCTAATAGGGCGTGTAGCAAGCTGTCATTTA TGCGAGGATCGAATACTCTGTTCACGACTGGTAGGCAGATAGGG-FAM
S3	CGCGACTGTCGCGTCAACTGCCTGCTGATATTCTACGTAACGGTCGAGGACTGCTCCGCTGATTC TAAGTAACGTATACTCGCTACGGCCGACTGGTAGGCAGATAGGG-FAM
S4	CGCTCTGCTGGACAGCAGACTGAGGAATGTTTTCAGCGGAGCAGTCCTCGACCGTTACGTAGTTC TGCCTGAACAGAGTATTCGATCCTCCGACTGGTAGGCAGATAGGG-FAM
S5	CCCTATCTGCCTACCAGTCG
Aptamer	CGACTGGTAGGCAGATAGGGGAAGCTGATTCGATGCGTGGGTCG

emission spectra of mixture were recorded with a scan range of 500–640 nm. All data were obtained from duplicate experiments (n = 5).

3. Results and discussion

3.1. Characterizations of GO and Au NPs-GO

The characteristic of the GO and Au NPs-GO were estimated using scanning electron microscopy (SEM) in Fig. 1A and B. The GO had a characteristic wrinkled layer nanostructure. And well dispersed, relatively uniform structured AuNPs were observed on the surface of GO. Meanwhile, the transmission electron micrograph (TEM) image of Au NPs was showed in Fig. 1C, which displayed a uniform spherical structure with an average diameter of 16 nm. This result was consistent with the Fig. 1D. Furthermore, zeta potential result showed the potential of Au NPs were positively charged in Fig. 1E. In addition, UV/vis absorption spectra provided the information about the formation of Au NPs-GO. As shown in Fig. 1F, a characteristic absorption peak of AuNPs obtained at 527 nm (curve b) after the formation of Au NPs-GO compared to GO (curve a). Meantime, XPS characterization was employed in Fig. 1G to provide additional evidence about the formation of Au NPs-GO, XPS peaks at 284.1 ev and 533.9 ev showed the positions of C1s and O1s of GO, while the XPS signature of Au 4f doublet at 84.1 ev and 87.8 ev illustrated the presence of metallic gold Au. High-resolution XPS spectra for Au, C, and O was in Fig. 1H–J.

3.2. Characterization of DTNs assembly

The construction of the DTNs assembly was verified by agarose gel electrophoresis. As depicted in Fig. 2A, lane 1 was DNA marker, lane 2, 3,4 and 5 at 94, 109, 109, and 109 bp showed the basic bases of S1, S2, S3 and S4, respectively. Lane 6 was loaded the upper supernatant of the centrifugal reaction products including S1, S2, S3 and S4. The featured and relatively slower migration bands in lane 6 indicated the formation of DTNs. Fig. 2B showed the structure of DTNs using AFM image, with an average diameter of 13.14 nm (Fig. 2C). Meanwhile, zeta potential result showed the potential of DTNs were negatively charged (Fig. 2D).

3.3. Feasibility of the sensor for serotonin detection

To evaluate the feasibility of the sensor for serotonin analysis, the fluorescence response of the sensor was detected. The excitation and emission wavelengths were set at 495 and 518 nm, the slit width for both excitation and emission was set at 5.0 nm. As displayed in Fig. 3, the formed DTNs exhibited obvious fluorescence signal at 521 nm for FAM. However, after the incubation of DTNs with Au NPs-GO (0.15 mg/mL), the fluorescence signal of FAM was effectively quenched by GO@AuNPs because of FRET effect from fluorescence molecules (donor) to Au NPs-GO (quencher) (curve a). When target serotonin presented with 500 pM and 10 nM, the fluorescence signal of FAM increased (curve b and c), demonstrating the effective hybridization of S5 with the single-strand DNA tails in DTNs, resulting in the release of DTNs from Au NPs-GO surface, which directly result in the recovery of the fluorescence signal of FAM.

3.4. Optimization of experimental conditions

To optimize the system for the detection of serotonin, the reaction time of aptamer with serotonin and S5 with DTNs was investigated. As shown in Fig. 4A, the fluorescence signal of FAM greatly increased with the increasing of reaction time of aptamer with serotonin, and a stable plateau was gradually reached after 40 min. Thus, 40 min was enough for subsequent experiments. Moreover, we also examined the reaction time of S5 with DTNs. As illustrated in Fig. 4B, the fluorescence signal of FAM increased and reached a plateau after 50 min. The result indicated that the reaction time between the DTNs and S5 was completed after 50 min.

3.5. Performance of the sensor for quantitative detection of serotonin

Under optimized experimental conditions, quantitative detection of serotonin was constructed using the proposed sensing platform. As shown in Fig. 5A, the fluorescence response gradually increased with the increasing of serotonin concentration from 0, 50 pM, 100 pM, 500 pM, 1 nM, 10 nM, 50 nM, 100 nM–200 nM. Meanwhile, the calibration plot for quantitative determination of serotonin was presented in Fig. 5B. The regression equation was expressed as $FL = 46.7 \log c + 233.19$ ($R^2 = 0.9946$) with a detection limit of 16.8 pM. In addition, specificity for serotonin assay was fatal to evaluate the performances of the sensor. As shown in Fig. 5C, the fluorescence response of the proposed method upon incubation with 50 nM of serotonin was obvious, while that for other interfering substances such as serum albumin, glutamic acid, epinephrine, and adenosine were similar to that of the blank, which illustrated that the proposed

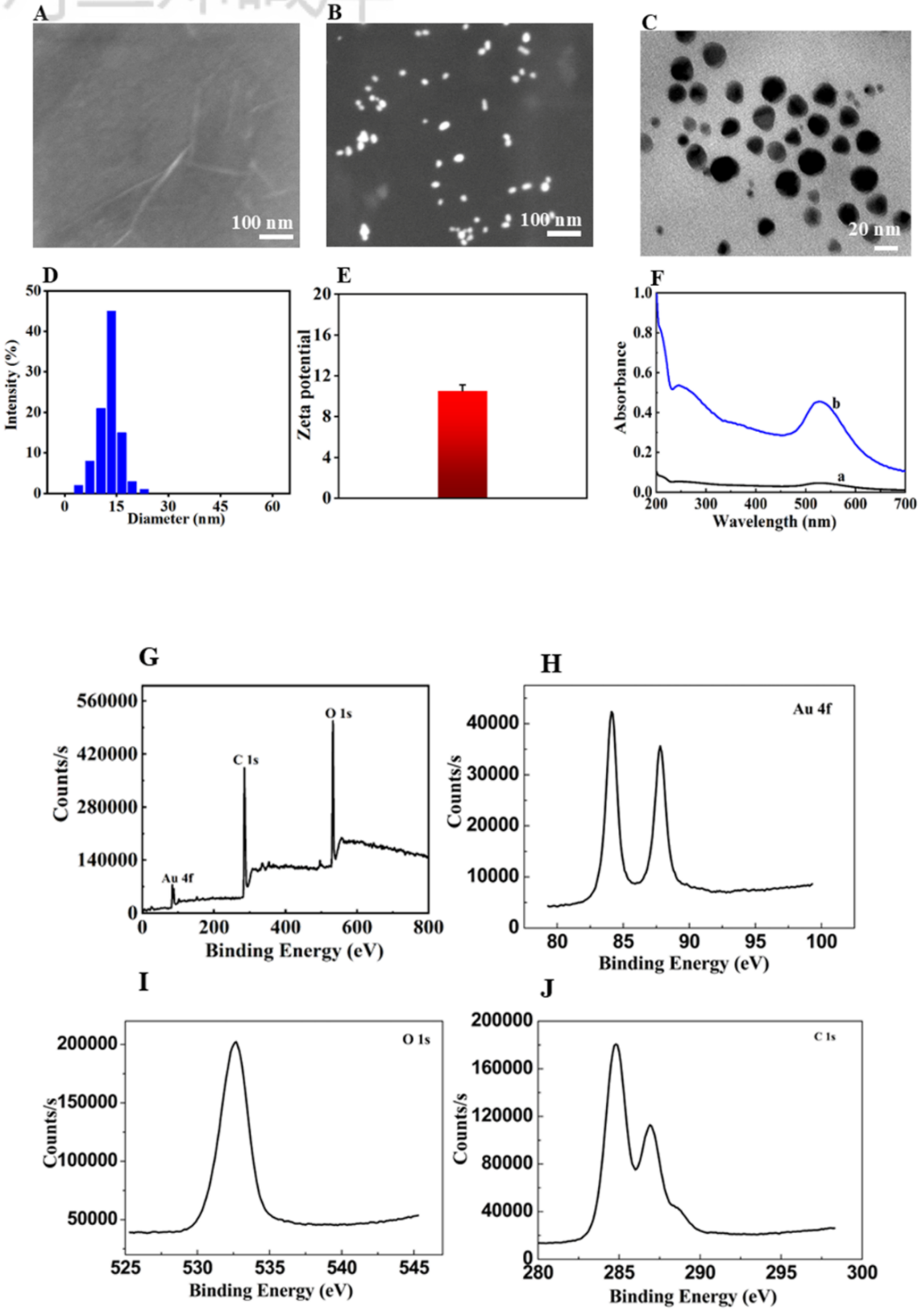

Fig. 1. (A) SEM image of GO; (B) SEM image of Au NPs-GO; (C) TEM image of Au NPs; (D) Diameter of Au NPs; (E) Zeta potential of Au NPs; (F) UV–vis absorption spectra of GO (a) and Au NPs-GO (b); (G) XPS analysis of Au NPs-GO; (H) XPS analysis of Au 4f; (I) XPS analysis of O 1S; (J) XPS analysis of C 1S.

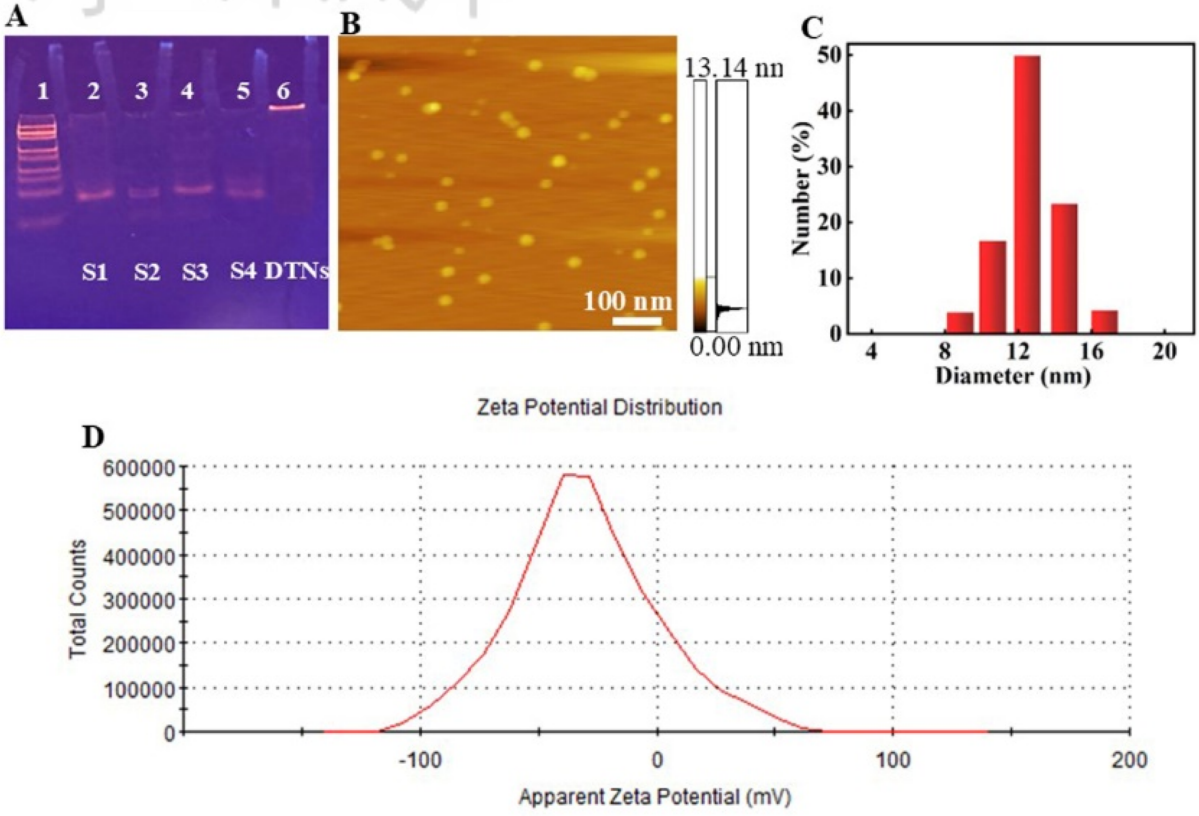

Fig. 2. (A) Polyacrylamide gel electrophoresis analysis of DTNs. Lane 1: DNA marker, lane 2: S1, lane 3: S2, lane 4: S3, lane 5: S3, lane 6: S1 + S2 + S3 + S4. (B) Atomic microscope of DTNs. (C) DLS diameter of DTNs. (D) Zeta potential of DTNs.

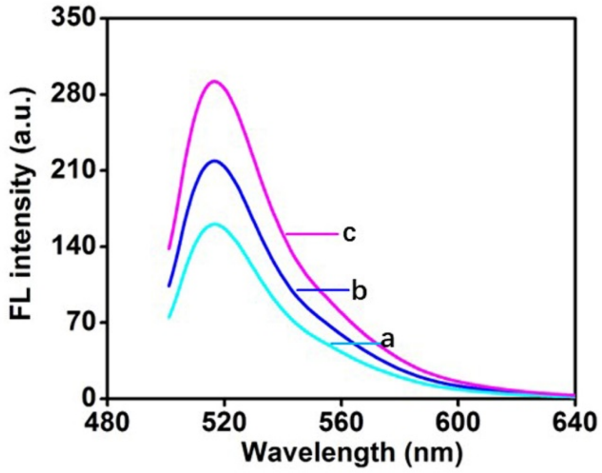

Fig. 3. Fluorescence spectral responses of GO@AuNPs/DTNs in the absence (a), presence of 500 pM (b) and 10 nM of serotonin (c).

method possesses high selectivity, and such high specificity of the sensor attributed to the highly specific binding ability of the aptamer with serotonin. Furthermore, in comparison with the results reported in previous work, the proposed method was comparable or possessed better analytical properties (Table 2).

3.6. Serotonin detection in human serum samples

In this work, to validate the practical applicability of the biosensor, serotonin detection was performed in healthy human serum samples, and the blood samples of healthy volunteer was collected from Heji Hospital Affiliated to Changzhi Medical College (Zhi Chang, China), followed by treating with centrifugation at 3000 r/min for 5 min. After being diluted 10-fold with PBS, 5, 50, and 100 nM serotonin was spiked into the above samples. Then, the serotonin was detected by using our proposed method. As shown in Table 3, the recoveries were obtained in the range from 99.49% to 100.80%, with the relative standard deviations (RSD) from 3.62% to 1.54%. Such result revealed that the proposed method possessed a good application prospect in human serum samples.

3.7. Conclusions

In summary, a sensitive fluorescent switching sensor was developed for the detection of serotonin. Taking advantages of Au NPs-GO as a fluorescence quencher, the background signal could be effectively

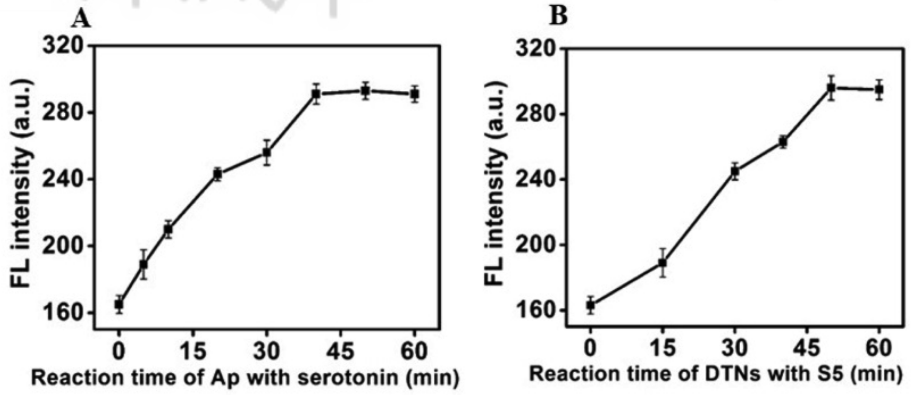

Fig. 4. The reaction time of aptamer with serotonin (A) and S5 with DTNs (B).

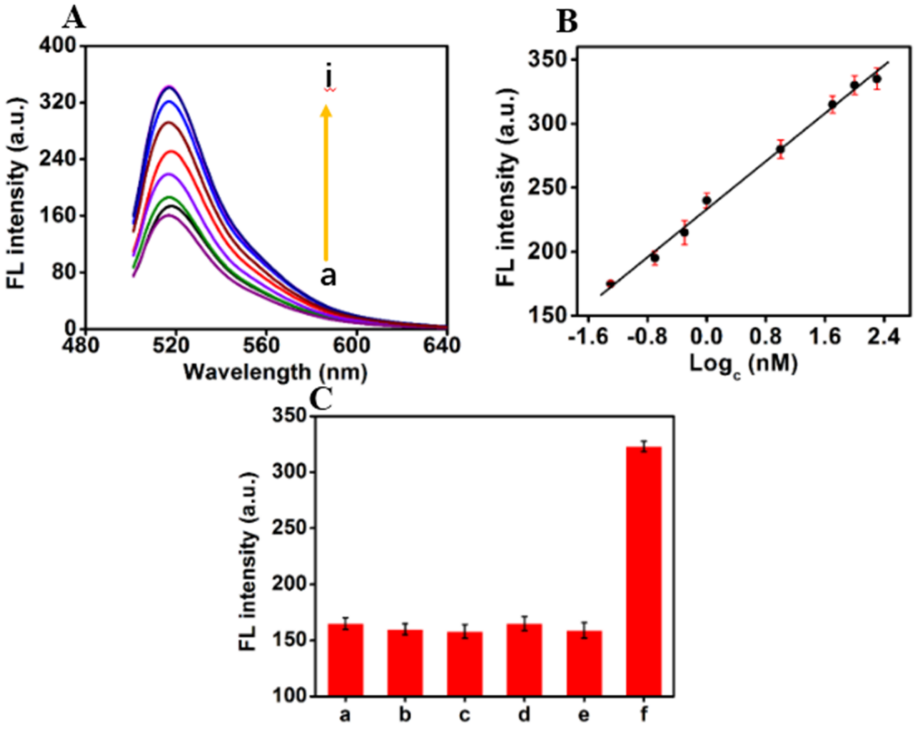

Fig. 5. (A) Fluorescence responses of the sensor to serotonin at concentrations varied from 0, 50 pM, 100 pM, 500 pM, 1 nM, 10 nM, 50 nM, 100 nM–200 nM (a–i); (B) The calibration curve of fluorescence intensity vs. logc serotonin; (C) Selectivity of the sensor against interfering substances (a–f: the blank solution, serum albumin, glutamic acid, epinephrine, adenosine, serotonin).

Table 2. Comparison of our proposed method with the previous works.

Method	Linear range	Detection limit	References
Fluorescence	0.2–1 μM	23.6 pM	[2]
ECL	1 pM – 1 μM	0.28 pM	[5]
Electrochemical	0 – 400 nM	0.9 nM	[6]
Electrochemical	0.1–800 μM	10 nM	[7]
ECL	5 pM–1 μM	1.5 pM	[8]
Ratiometric SERS	5×10^{-7}–1×10^{-3} M	4.9×10^{-9} M	[11]
Fluorescence	50 pM–200 nM	16.8 pM	This work

Table 3. Addition and recovery experiments of serotonin in human serum samples.

Samples	$c_{serotonin}$ (nM)	Added (nM)	Measured (nM)	Recovery (%)	RSD (%, n = 5)
Human serum 1	0.93	5	5.98	100.8	3.62
Human serum 2	1.12	50	50.86	99.49	2.73
Human serum 3	1.16	100	101.32	100.15	1.54

reduced, which can guarantee the reliability of sensing system. Meanwhile, when the aptamer reacted with serotonin, three double-stranded DNA products were formed and the adsorption effect of Au NPs-GO could be eliminated. Moreover, the use of aptamer endowed this sensing system high specificity toward target serotonin against other interfering substances such as serum albumin, glutamic acid, epinephrine, and adenosine. Furthermore, this strategy could effectively reduce the false-positive signal, accordingly improved the accuracy of the method in serotonin detection.

Acknowledgements

We gratefully acknowledge Basic Research Program of Shanxi Province (Free Exploration No. 20210302124696, No. 202203021222309 and No. 202403021211134).

References

[1] Basu S, Hendler-Neumark A, Bisker G. Role of oxygen defects in eliciting a divergent fluorescence response of single walled carbon nanotubes to dopamine and serotonin. ACS Nano 2024;18:34134–46.
[2] Zhang SY, Song GG, Yang Z, Kang K, Liu XQ. A label-free fluorescence aptamer sensor for point-of-care serotonin detection. Talanta 2024;277:126363–71.
[3] Chavan SG, Rathod PR, Koyappayil A, Wang SH, Lee MH. Recent advances of electrochemical and optical point-of-care biosensors for detecting neurotransmitter serotonin biomarkers. Biosens Bioelectron 2025;267:116743–71.
[4] Wang ZH, Zhang YF, Zhang B, Lu XQ. Mn^{2+} doped ZnS QDs modified fluorescence sensor based on molecularly imprinted polymer/sol-gel chemistry for detection of serotonin. Talanta 2018;190:1–8.
[5] Li HY, Jiao Y, Shi YB, Feng QM, Gao YG. Bipedal DNA walker integrated resonance energy transfer to construct a sensitive electrochemiluminescence biosensor for serotonin detection. Talanta 2025;293:128175–82.
[6] Chavan SG, Yagati AK, Koyappayil A, Go A, Yeon S, Lee T, et al. Conformationally flexible dimeric-serotonin-based sensitive and selective electrochemical biosensing strategy for serotonin recognition. Anal Chem 2022;94:17020–30.
[7] Nehru L, Chinnathambi S, Fazio E, Fortunato N, Leonardi SG, Bonavita A, et al. Electrochemical sensing of serotonin by a modified MnO2-graphene electrode. Biosen 2020;10:33–45.
[8] Gao YG, Feng QM, Miao XM, Fu YF. An in situ-boosted electrochemiluminescence biosensor for serotonin detection sensitized with Co_3O_4 nanoplates and self-feedback DNA recycling. Biosens Bioelectron 2025;281:117464–71.
[9] Guo Y, Xu Y, Wu M, Feng Q. Resonance energy transfer-based electrochemiluminescence aptasensor for serotonin detection. Talanta 2025;281:126888.
[10] Chavan SG, Yagati AK, Kim HT, Jin E, Park SR, Patil DV, et al. Dimeric-serotonin bivalent ligands induced gold nanoparticle aggregation for highly sensitive and selective serotonin biosensor. Biosens Bioelectron 2021;19:1113447–56.
[11] Fan M, Han SR, Huang Q, Chen JB, Feng SY, Lu YD, et al. Ratiometric SERS-based assay with "sandwich" structure for detection of serotonin. Microchim Acta 2023;190:3–10.
[12] Sha Q, Sun B, Yi C, Guan R, Fei J, Hu Z, et al. A fluorescence turn-on biosensor based on transferrin encapsulated gold nanoclusters for 5-hydroxytryptamine detection. Sensor Actuat B-Chem 2019;29:4177–84.
[13] Kelich P, Jeong S, Navarro N, Adams J, Sun X, Zhao H, et al. Discovery of DN-carbon nanotube sensors for serotonin with machine learning and near-infrared fluorescence spectroscopy. ACS Nano 2021;16:736–45.
[14] Zhang Y, Gao L, Han J, Miao XM. Dual-signal and one-step monitoring of Staphylococcus aureus in milk using hybridization chain reaction based fluorescent sensor. Spectrochim Acta Mol Biomol Spectrosc 2023;303:123191–8.
[15] Yin KP, Wu SQ, Zheng H, Gao L, Liu JF, Yang CL, et al. Lanthanide metal–organic framework-based fluorescent sensor arrays to discriminate and quantify ingredients of natural medicine. Langmuir 2021;37:5321–8.
[16] Raghavan VS, O'Driscoll B, Bloor JM, Li B, Katare P, Sethi J, et al. Emerging graphene-based sensors for the detection of food adulterants and toxicants-A review. Food Chem 2021;355:129547–62.
[17] Shen W, Wang C, Zheng S, Jiang B, Li J, Pang Y, et al. Ultrasensitive multichannel immunochromatographic assay for rapid detection of foodborne bacteria based on two-dimensional film-like SERS labels. J Hazard Mater 2022;437:129347–58.
[18] Tian JQ, Tu QC, Li MY, Zhao LJ, Zhu YD, Lee JH, et al. Development of fluorescent GO-AgNPs-Eu^{3+} nanoparticles based paper visual sensor for foodborne spores detection. Food Chem 2024;21:101069–79.
[19] Kasputis T, He YW, Ci QQ, Chen JH. On-site fluorescent detection of sepsis-inducing bacteria using a graphene-oxide CRISPR-Cas12a (GO-CRISPR) system. Anal Chem 2024;96:2676–83.
[20] Sun P, Xu KB, Guang SY, Xu HY. Monodisperse functionalized GO for high-performance sensing and bioimaging of Cu^{2+} through synergistic enhancement effect. Talanta 2021;24:121786–98.
[21] Kalkal A, Pradhan R, Packirisamy G. Gold nanoparticles modified reduced graphene oxide nanosheets based dual-quencher for highly sensitive detection of carcinoembryonic antigen. Int J Biol Macromol 2023;242:125157–66.
[22] Abi A, Lin MH, Pei H, Fan C, Ferapontova EE, Zuo XL. Electrochemical switching with 3D DNA tetrahedral nanostructures self-assembled at gold electrodes. ACS Appl Mater Interfaces 2014;6:8928–31.
[23] Jia RC, He XX, Ma WJ, Lei YL, Cheng H, Sun H, et al. Aptamer-functionalized activatable DNA tetrahedron nanoprobe for PIWI-interacting RNA imaging and regulating in cancer cells. Anal Chem 2019;91:15107–13.
[24] Wang J, He YH, Liu LY, Chen XJ, Hou XQ, Wang JX, et al. DNA tetrahedron-based dual-signal fuorescence detection of apoE4 gene sites on a microplate reader. Microchim Acta 2024;191:288–96.
[25] Ren WJ, Pang JR, Ma RR, Liang XJ, Wei M, Suo ZG, et al. A signal on-off fluorescence sensor based on the self-assembly DNA tetrahedron for simultaneous detection of

ochratoxin A and aflatoxin B1. Anal Chim Acta 2022;1198: 339566–76.

[26] Zhao XS, Xu Y, Chen ZT, Tang CG, Mi XQ. Encoding fluorescence intensity with tetrahedron DNA nanostructure based FRET effect for bio-detection. Biosens Bioelectron 2024;248:115994–6001.

[27] Ye T, Xu YM, Chen HH, Yuan M, Gao H, Wu XX, et al. A trivalent aptasensor by using DNA tetrahedron as scaffold for label-free determination of antibiotics. Biosens Bioelectron 2024;251:116127–35.

[28] Su XY, Chen ZY, Wang H, Yuan L, Zheng KY, Zhang W, et al. Ratiometric immunosensor with DNA tetrahedron nanostructure as high-performance carrier of reference signal and its applications in selective phoxim determination for vegetables. Food Chem 2022;383:132445–54.

[29] Li ZB, Xu HW, Feng QM, Zhang ZF, Miao XM. Two-step förster resonance energy transfer amplification for ratiometric detection of pathogenic bacteria in food samples. Food Chem 2023;404:134492–9.

[30] Yang MC, Hardiansysh A, Cheng YW, Liao HL, Wang KS, Randy A, et al. Reduced graphene oxide nanosheets decorated with core-shell of Fe_3O_4-Au nanoparticles for rapid SERS detection and hyperthermia treatment of bacteria. Spectrochim Acta Mol Biomol Spectrosc 2022;281: 121578–87.

[31] Miao XM, Xiong C, Wang WW, Li LS, Shuai XT. Dynamic-light-scattering-based sequence-specific recognition of double-stranded DNA with oligonucleotide-functionalized gold nanoparticles. Chem Eur J 2011;17: 11230–6.